Applied Energy 254 (2019) 113636

Contents lists available at ScienceDirect

Applied Energy

journal homepage: www.elsevier.com/locate/apenergy

Potential of renewable fuel to reduce diesel exhaust particle emissions

Liisa Pirjola[a,b,*], Heino Kuuluvainen[c], Hilkka Timonen[d], Sanna Saarikoski[d], Kimmo Teinilä[d], Laura Salo[c], Arindam Datta[e], Pauli Simonen[c], Panu Karjalainen[c], Kari Kulmala[f], Topi Rönkkö[c]

[a] Department of Automotive and Mechanical Engineering, Metropolia University of Applied Sciences, P.O. Box 4071, FI-01600 Vantaa, Finland
[b] Department of Physics, University of Helsinki, P.O. Box 64, 00014 Helsinki, Finland
[c] Aerosol Physics Laboratory, Physics Unit, Tampere University, P.O. Box 692, FI-33101 Tampere, Finland
[d] Atmospheric Composition Research, Finnish Meteorological Institute, P.O. Box 503, FI-00101 Helsinki, Finland
[e] The Energy and Resources Institute, New Delhi, India
[f] Neste Oyj, P. O. Box 95, FI-00095 Neste, Finland

HIGHLIGHTS

- Exhaust emissions from a current Indian standard diesel vehicle were investigated.
- Particle size distributions, BC content and chemical mass composition were measured.
- Emissions were compared during NEDC and WLTC with three fuels.
- Emissions characteristics were strongly dependent on the fuels and driving conditions.
- The lowest BC emissions were obtained with sulphur- and aromatic-free renewable diesel.

GRAPHICAL ABSTRACT

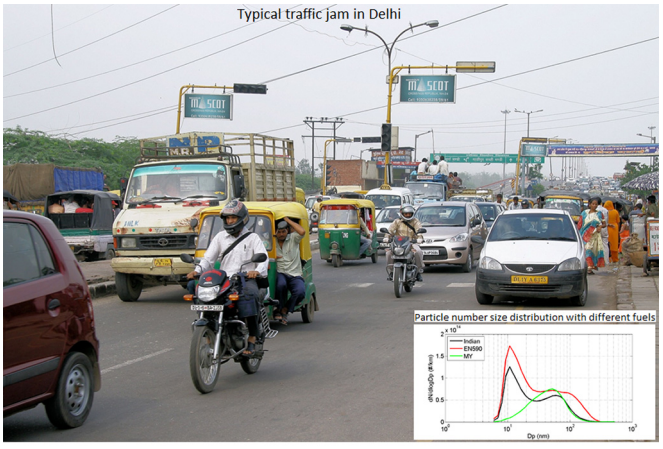

Photo: Timo Anttila

ARTICLE INFO

Keywords:
Renewable fuel
Combustion
Traffic emissions
New European Driving Cycle
Worldwide harmonized Light vehicles Test Cycle
Black carbon

ABSTRACT

The use of fossil fuels in traffic is a significant source of air pollutants and greenhouse gases in rapidly growing and densely populated cities. Diesel exhaust emissions including particle number concentration and size distribution along with the particles' chemical composition and NOx were investigated from a Euro 4 passenger car with a comprehensive set of high time-resolution instruments. The emissions were compared with three fuel standards – European diesel (EN590), Indian diesel (BS IV) and Finnish renewable diesel (Neste MY) – over the New European Driving Cycle (NEDC) and the Worldwide harmonized Light vehicles Test Cycle (WLTC). Fuel properties and driving conditions strongly affected exhaust emissions. The exhaust particulate mass emissions for all fuels consisted of BC (81–88%) with some contribution from organics (11–18%) and sulfate (0–3%). As aromatic-free fuel, the MY diesel produced around 20% lower black carbon (BC) emissions compared to the EN590 and 29–40% lower compared to the BS IV. High volatile nanoparticle concentrations at high WLTC speed conditions were observed with the BS IV and EN590 diesel, but not with the sulfur-free MY diesel. These nanoparticles were linked to sulfur-driven nucleation of new particles in cooling dilution of the exhaust. For all the

* Corresponding author at: Department of Automotive and Mechanical Engineering, Metropolia University of Applied Sciences, P.O. Box 4071, FI-01600 Vantaa, Finland.
E-mail address: liisa.pirjola@helsinki.fi (L. Pirjola).

https://doi.org/10.1016/j.apenergy.2019.113636
Received 27 May 2019; Received in revised form 22 July 2019; Accepted 30 July 2019
0306-2619/ © 2019 Metropolia University of Applied Sciences. Published by Elsevier Ltd. This is an open access article under the CC BY-NC-ND license (http://creativecommons.org/licenses/BY-NC-ND/4.0/).

fuels non-volatile nanoparticles in sub-10 nm particle sizes were observed during engine braking, and they were most likely formed from lubricant-oil-originated compounds. With all the fuels, the measured particulate and NOx emissions were significantly higher during the WLTC cycle compared to the NEDC cycle. This study demonstrated that renewable diesel fuels enable mitigations of particulate and climate-warming BC emissions of traffic, and will simultaneously help tackle urban air quality problems.

1. Introduction

Combustion of fossil fuels is a significant anthropogenic source for greenhouse gases (GHG) (CO_2, CH_4, N_2O, O_3, NOx) and black carbon (BC) emissions causing climate warming [1–3]. In 2016 direct CO_2 emissions of transport sector (road, air, water, other) worldwide were 32.3 $GtCO_2$/yr, of which road sector (i.e., diesel fuel combustion) accounted for 74% being 18% of global CO_2 emissions [4]. Around 30% of road sector emissions were generated in America and 30% in Asia. Additionally, particulate matter from diesel emissions contain carcinogenic and mutagenic agents, and they have been linked to increased complications in cardiovascular and respiratory systems [5–11].

The combustion processes in diesel engines produce a complex mixture of gaseous and particulate emissions [12]. Particulate emissions can be divided into three types according to their formation mechanisms: (1) Primary emissions are formed in the engine. Primary particles are soot particles, composed of non-volatile carbonaceous soot agglomerates [13,14] and small particles possessing non-volatile cores (< 10 nm in size) that have been observed in some driving conditions [14–16]. The origins of these particles are fuel aliphatic hydrocarbons [17] and lubricant oil metal compounds [18–20]. (2) Fresh emissions contain the abovementioned primary particles and the particulate matter formed in the atmosphere during rapid cooling and dilution of the exhaust; that is, semi-volatile compounds that can condense onto the surfaces of primary particles or nucleate and form new particles in less than 1 s atmospheric residence time when H_2SO_4-H_2O nucleation takes place [15,21–26]. The nucleated particles consist of volatile materials such as water, sulfate, and hydrocarbons [12]. (3) Secondary organic aerosol (SOA) is formed in the atmosphere due to the effects of oxidants and UV light on precursor gases emitted by vehicles. In this process, high vapour pressure organic compounds oxidize into low-volatility compounds which then can form SOA via gas-to-particle conversion [27,28].

Due to their adverse health effects and climate-warming potential, the emissions of diesel vehicles are regulated. In 2014, stringent regulations for new diesel passenger cars were implemented in Europe (Euro 6 standards) and in the USA (EPA Tier 3 regulations) [29]. Fuel sulfur content (FSC) less than 10 ppm (weight) for diesel fuels became mandatory in the EU from 2009, and less than 15 ppm in the USA from 2006. Since September 2018, all new vehicles in the EU must be certified according to the new Worldwide harmonized Light vehicles Test Cycle (WLTC) chassis dynamometer procedure, which replaced the earlier New European Driving Cycle (NEDC) test. The WLTC simulates real driving conditions better than the NEDC. Furthermore, since 2017, in addition to laboratory testing of Euro 6 standards, real driving emissions (RDE) road test must be performed using a portable emissions monitoring system (PEMS) to control vehicle emissions in real operation [29]. Developing countries follow the legislation of the EU and the USA. For example, in 2000, India began adopting European emission and fuel regulations for four-wheeled light-duty and heavy-duty vehicles. BS IV standards, corresponding to the Euro 4, have been enforced for the entire country since April 2017, and India would adopt the BS VI standards (Euro 6) in 2020. The diesel fuel sulfur content (FSC) was reduced from 2500 ppm to 50 ppm nationwide in 2017 (BS IV standards). The FSC specifications call for sulfur reductions down to 10 ppm with the introduction of BS VI in 2020.

To meet the Euro 6 regulations, new diesel vehicles need to be equipped by after-treatment systems (ATS) such as diesel oxidizing catalysts (DOCs), particulate filters (DPFs) and selective catalyst reduction (SCR) systems. It should be noted that the countries with less restrictive emission legislation still have a large number of diesel vehicles without these advanced ATS, and that the renewal of vehicle fleet is a very slow process. However, alternative fuels, such as biodiesel (FAME) and renewable fuel (hydrotreated vegetable oil, HVO), ethanol, vegetable oils, and their blends with diesel fuel, have recently been developed and used in diesel engines. Details of biofuels are presented in Section 2. A DOC is used to remove hydrocarbons and CO, a DPF to trap PM, and a SCR or a NOx adsorption catalyst to remove NOx. Unfortunately, DOCs simultaneously increase SO_2 to SO_3 conversion enhancing gaseous sulfuric acid formation [21,22]. Sulfuric acid has been shown to participate in condensation and nucleation processes during the dilution and cooling of the exhaust [21,22,18,23–26]. Physicochemical properties of diesel exhaust emissions significantly depend on engine and after-treatment technology as well as used fuel [30–32,28,33] and lubricant oil [34,35]. Furthermore, driving conditions [36] and temperature of the engine (i.e. cold start) have been shown to significantly influence the concentration and composition of emissions [37]. More details on the physical and chemical characteristics of regulated diesel exhaust emissions can be found in the review papers by Burtscher [38], Maricq et al. [32], Myung et al. [39], and Choi et al. [40].

Only a limited number of studies yet exist concerning diesel exhaust emissions over the WLTC; most of them deal with gaseous emissions [41–46]. Many aspects of diesel exhaust emissions remain poorly characterized, especially the influence of real-driving conditions to emissions, influence of biofuels to composition of emissions as well as to nanoparticle emissions. The novelty of this paper lies on investigating the potential of renewable fuel compared to European and Indian diesel fuels to reduce the climate and air quality influencing particle emissions, especially regarding (but not limited to) Indian diesel-powered traffic. The number of particle emissions and size distributions together with their chemical composition were studied over the WLTC by a comprehensive set of high-time-resolution instruments. More detailed objectives are (i) to quantitatively investigate the influence of different fuels including HVO and two commercial fossil fuels on exhaust emissions, (ii) to study primary and freshly emitted PM and gaseous compounds from a representative Indian diesel passenger car (Euro 4) under laboratory conditions, and (iii) to identify differences in particulate emissions due to different driving conditions over the NEDC and WLTC cycles.

2. Renewable biofuels

To mitigate the climate change, alternative fuels with less environmental impacts are needed to replace the use of fossil fuels. Low-carbon fuels, especially different types of biofuels have been developed. For example, biodiesel is produced from vegetable oils by esterification and the products are called fatty acid methyl esters (FAME). Hydrotreated vegetable oil (HVO) is a renewable diesel fuel whose feedstock are vegetable oils (rapeseed, sunflower, soybean, palm, jatropha and algae oils) and waste animal fats. E.g. in Neste MY renewable diesel, at least 80% of renewable raw material is waste and residues. In the production process, hydrogen is used to remove the oxygen from the vegetable oil after which catalytic isomerization into branched alkanes is done to get paraffinic hydrocarbons. Consequently, HVO is practically free of metals and ash-forming elements.

Concerning energy conversion, GHG emissions (in gCO2eq/km) and energy use (in MJ/100 km) are the most important aspects in life cycle assessment (LCA) of fuels. Total energy use covers fossil energy consumption during all life cycle phases, i.e. feedstock production and transportation to refineries, fuel refining and transportation to distribution stations, and fuel combustion [47,48]. Edwards et al. [49] estimated 45–75% fossil energy saving for biodiesel and 79% saving for HVO compared to conventional diesel fuel. In addition, the GHG emission saving was 40–70% for biodiesel, 42% for HVO and 50–90% for the MY. On the other hand, Arvidsson et al. [47] estimated somewhat higher total energy use for HVO when biomass energy losses, i.e. inefficiencies in the use of biomass feedstock in the production of biofuels, were included. However, in their study the GHG emissions for HVO were 30% lower than for diesel. IPCC [1] reports that biofuels have 30–90% lower GHG emissions than diesel fuels; however, indirect emissions from land use and change are not well known [50].

Although the heating value of HVO per mass (~44 MJ/kg) is somewhat higher than that for EN590 diesel (~42.7 MJ/kg), the volumetric fuel consumption of HVO is higher due to its lower density leading to a slightly lower volumetric heating value of 34.4 MJ/dm^3 compared to 35.7 MJ/dm^3 for EN590. However, HVO has higher energy content compared to FAME. Nylund et al. [51] reported that during their bus tests HVO increased fuel consumption by 5.2% and FAME around 9% in maximum compared to fossil diesel with no bio-component.

Nevertheless, HVO has many beneficial properties to the engine, ATS and environment. Practically all new diesel cars are equipped with a diesel catalyst system and a DPF. The functioning of DPF depends on the composition of soot particles in diesel exhaust, and the type of soot depends on the fuel used. Renewable fuels have higher cetane number paraffinic hydrocarbons that are free of aromatics and sulfur, and therefore produce less particulate emissions enabling longer regeneration frequency and, consequently, lower fuel consumption [52]. As HVO is sulfur-free, harmful SO_2 oxidation to SO_3 in DOCs is limited reducing particle number and mass emissions formation. Additionally, undesirable storage of sulfur compounds in the DOC that decreases the DOC oxidation power ("sulfur poisoning") and thus increases emissions of gaseous hydrocarbon compounds [53], does not exist for HVO. Use of HVO has been shown to reduce GHG emissions, CO, and total hydrocarbon (THC) emissions as well as soot emissions [54,55,22,56,51,57].

3. Experimental setup

3.1. Tested vehicle, lubricant oil and fuel properties

The tested diesel vehicle was a Euro 4 Toyota Corolla 2.2 D-4D (4 cylinders, displacement 2.2 dm^3, model year 2007, maximum power 100 kW), equipped with a DOC. The engine had a common rail direct injection system. The used engine oil was fully synthetic high performance motor oil Neste City Pro LL 5 W-30 (Supplementary Table S1), developed for extended oil drain intervals for passenger cars and vans. Excellent cold start properties provide easy cold starts under all operating conditions.

Three types of diesel were used in the experiments: (i) Indian diesel (BS IV) with FSC of 34.7 mg/kg, (ii) European commercial diesel (EN590) with FSC of 6.1 mg/kg, and (iii) renewable diesel (Neste MY) with FSC less than 1 mg/kg. The main differences between the fuels were in sulfur content, aromatic hydrocarbons and cetane number. Higher cetane helps an engine start in colder conditions and decreases exhaust emissions. The detailed fuel properties are given in Supplementary Table S2.

3.2. Driving modes

The measurements were conducted with the standardized NEDC (duration 1180 s, 10.9 km) and the WLTC (1800 s, 22.3 km). The NEDC is composed of four urban-like sub-cycles constituting the urban driving cycle (UDC) with a total duration of 780 s, followed by a 400 s long extra-urban driving cycle (EUDC). The UDC simulates city driving and is characterized by low engine load, low exhaust gas temperature, and an average speed of 18.4 km/h, whereas the EUDC simulates highway driving with an average speed of 62.6 km/h. The WLTC is composed of four phases including different maximum speeds and highly varying accelerations. The average speed during the low phase (589 s) is 19.0 km/h, during the medium phase (433 s) 39.4 km/h, during the high phase (455 s) 53.7 km/h, and during the extra-high phase (323 s) 89.4 km/h. More information on the phases is given in Supplementary Table S3. The WLTC simulates real driving conditions better than the NEDC.

The vehicle was soaked overnight (at least 8 h) at 20 °C prior to the cycles. The first driven cycle of each day is hereafter named the "cold start cycle". After the cold start cycle, the cycle was repeated three times, and all of these were considered "hot start cycles". One of the hot start cycles was measured for primary emissions (see Section 3.3), and two for fresh emissions and these two results were averaged. Before

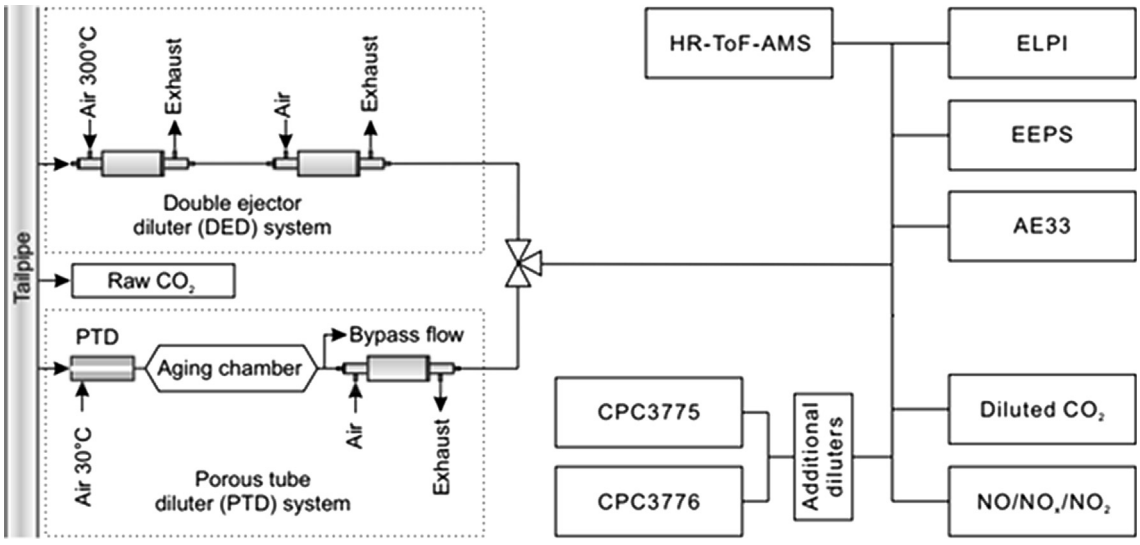

Fig. 1. Schematic of the experimental setup.

each hot start cycle, the engine was run for 10 min at 80 km/h to ensure sufficient warming of the engine, indicated by a coolant temperature of ~100 °C.

3.3. Exhaust sampling and instrumentation

The measurement setup is shown in Fig. 1. Particle sampling was conducted with two different partial flow dilution systems at the exhaust transfer line, with (1) a system [58] measuring the fresh emissions and (2) a double-ejector diluter system measuring the primary emissions. In both of the systems, the raw exhaust sample flow was nearly constant, ~5 L min^{-1} in the fresh emission measurements and ~4 L min^{-1} in the primary emission measurements. In the first case, the sampling system consisted of a porous tube diluter (PTD) with a dilution ratio (DR) of about 12, a short ageing chamber with a residence of 2.5 s, and a secondary diluter, a Dekati Diluter (Dekati Ltd.) with a DR of ~8. By this system the exhaust is diluted to a ratio of ~100, whereas in atmospheric conditions it might be even more than 1000 at plume ages of 2.7 s [19,59]. However, the nucleation mode is fully formed at a dilution ratio of approximately 100 [60], or after less than 0.7 s residence time in the atmosphere [15]. From the nucleation point of view, this system mimics atmospheric dilution and particle formation in roadside environments.

In the second case, the exhaust was diluted by double ejector diluters (DED) (Dekati Ltd.), the first of which was heated to ~300 °C. After the second ejector, the sample temperature was around 25–30 °C. Heating of the dilution air in the first ejector diluter prevents new particle formation; thus, the particles measured downstream in the sampling system represent primary particles. Pressurized dilution air was purified of particles and gaseous contaminants. The dilution ratios were calculated based on the measurements of the raw CO_2 concentration in the tailpipe and the diluted CO_2 concentration. The raw CO_2 concentration was measured with a specific PEMS CO_2 analyser. The diluted concentration was monitored with a LI-COR LI-840A gas

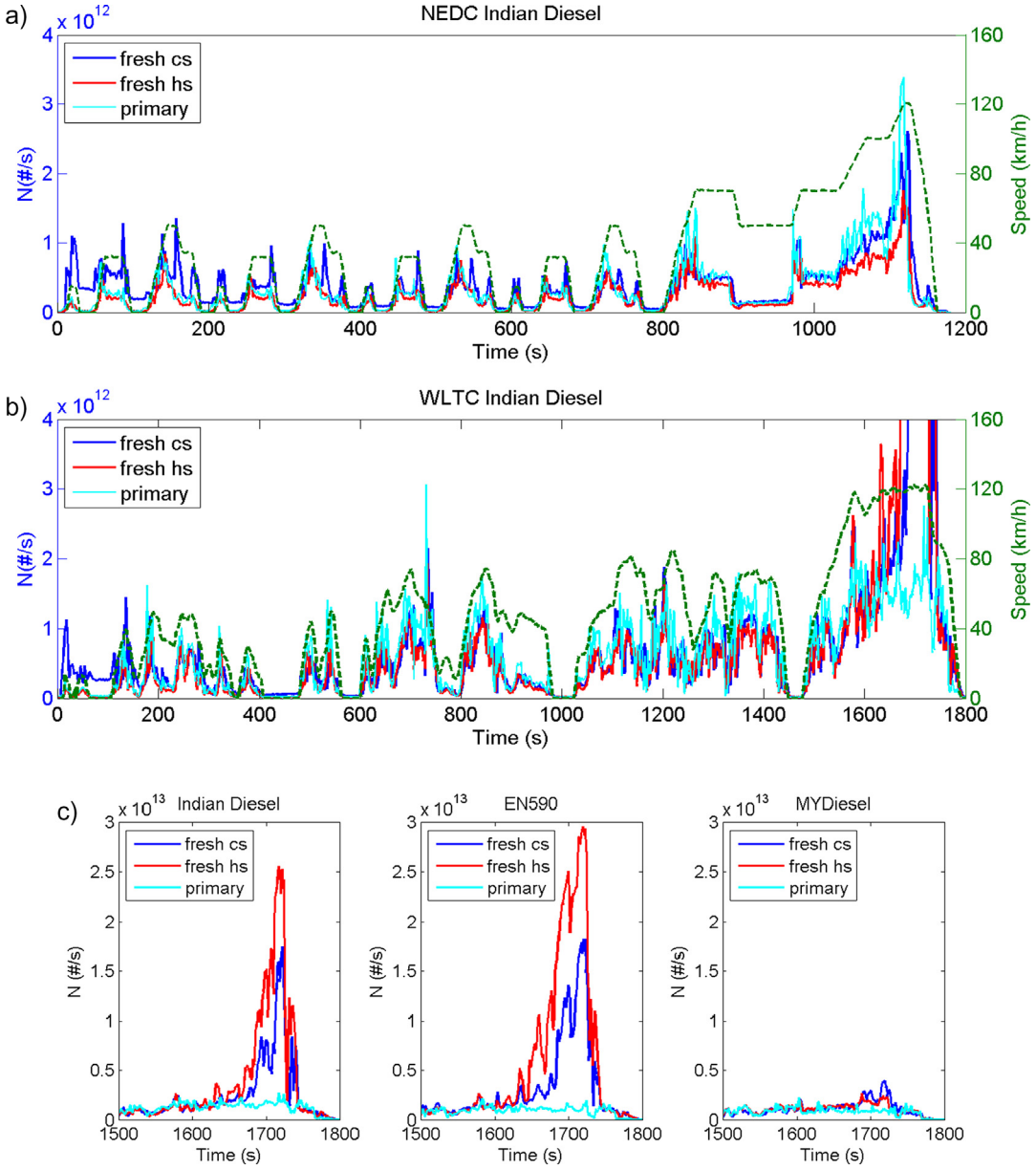

Fig. 2. Primary and fresh (hs = hot start, cs = cold start) particle emissions (measured by UCPC) during the NEDC (a) and WLTC (b) cycles when the vehicle was fuelled by Indian diesel (BS IV). Also shown are the vehicle speed profiles. Note that the peak emissions of the cs and hs curves at the extra-high speed phase of the WLTC are as high as 1.8×10^{13} and 2.6×10^{13} #/s, respectively. The subplots (c) show the extra-high phase emissions for all fuels.

analyser or with a SIDOR SICK MAIHAK gas analyser.

The distribution of the size of exhaust particles was measured with a time resolution of 1 Hz in the size range of 5.6–560 nm (mobile diameter) with an engine exhaust particle sizer (EEPS; TSI Inc.) [61], and in the size range of 7 nm–10 μm (aerodynamic diameter) with electrical low-pressure impactors (ELPI, Dekati Ltd) [62]. The ELPI was equipped with a filter stage [63] and an additional impactor stage designed for nanoparticles [64]. The particle concentration was measured with ultrafine condensation particle counters (UCPC3776 and UCPC3775, TSI Inc.) downstream of two additional diluters (bridge diluters with minimized losses for nanoparticles, total DR ~ 330) to ensure that the concentrations were in the operational range of the UCPC.

The black carbon (BC) in the PM_1 size fraction was measured by a 7-wavelength (370, 470, 520, 590, 660, 880, and 950 nm) aethalometer (AE 33, Magee Scientific) with a time resolution of 1 s. The AE 33 uses the dual-spot method to compensate for the "spot loading effect", and gives a compensated BC concentration and a loading compensation parameter for each wavelength. The missing BC concentrations due to tape advances (~5 min) were measured using another similar aethalometer (AE33) installed in parallel to the AMS (not shown in Fig. 1). The absorption at the wavelengths 880 and 370 nm was converted to BC and BrC using mass-absorption cross section values given by the manufacturer.

A soot particle aerosol mass spectrometer (SP-AMS, Aerodyne Research Inc., [65]) was used to study the influence of fuel and driving cycle on temporal variations in particle chemistry. The SP-AMS has a dual vaporizer system in which, in addition to the normal tungsten oven, an intracavity Nd:YAG laser (1064 nm) vaporizer is added, into high resolution time-of-flight aerosol mass spectrometer (HR-ToF-AMS, [66]). The dual vaporizer enables measurements of refractory black carbon (rBC) and associated refractory particulate material (e.g., metals) in addition to non-refractory species such as sulfate (SO_4), nitrate (NO_3), ammonium (NH_4), chloride (Cl) and organics (Org). In this study, SP-AMS was measured in a mass spectrum (MS) mode mostly with ~8 s time resolution, but due to software-related issues during some cycles, a higher time resolution was used (up to 20 s). The data shown in this paper for organic and inorganic species were measured with the laser off only. A PM_1 cyclone was inline in front of the SP-AMS, but the real measured particle size range was limited by an AMS aerodynamic lens between ~50 to 800 nm. The SP-AMS data were analysed using standard AMS data analysis software (SQUIRREL v1.57 and PIKA v1.16) within Igor Pro 6 (Wavemetrics, Lake Oswego, OR). The mass concentrations from the SP-AMS were calibrated with 300 nm ammonium nitrate particles, and data were calculated by using a default collection efficiency of 0.5 [67] and references therein. Due to a technical issue in the SP-AMS, the measurement results were only available for both cycles for the Indian diesel and MY diesel with the PTD dilution system.

Gaseous concentrations of nitrogen oxides NO, NO_2 and NOx (model APNA 360, Horiba) were also monitored downstream of the diluters with a time resolution of 1 s.

All the data shown below have been corrected by a total dilution ratio for each instrument representing the raw exhaust concentrations. To calculate the emissions (#/s for particle number and g/s for masses), the instantaneous concentrations were multiplied by the measured instantaneous exhaust flow volume (the air density was assumed to be 1.2 kg/m^3). The emissions factors (#/km, g/km) were then obtained by dividing the combined emissions over the cycles by the combined speed (km/s) over the cycles.

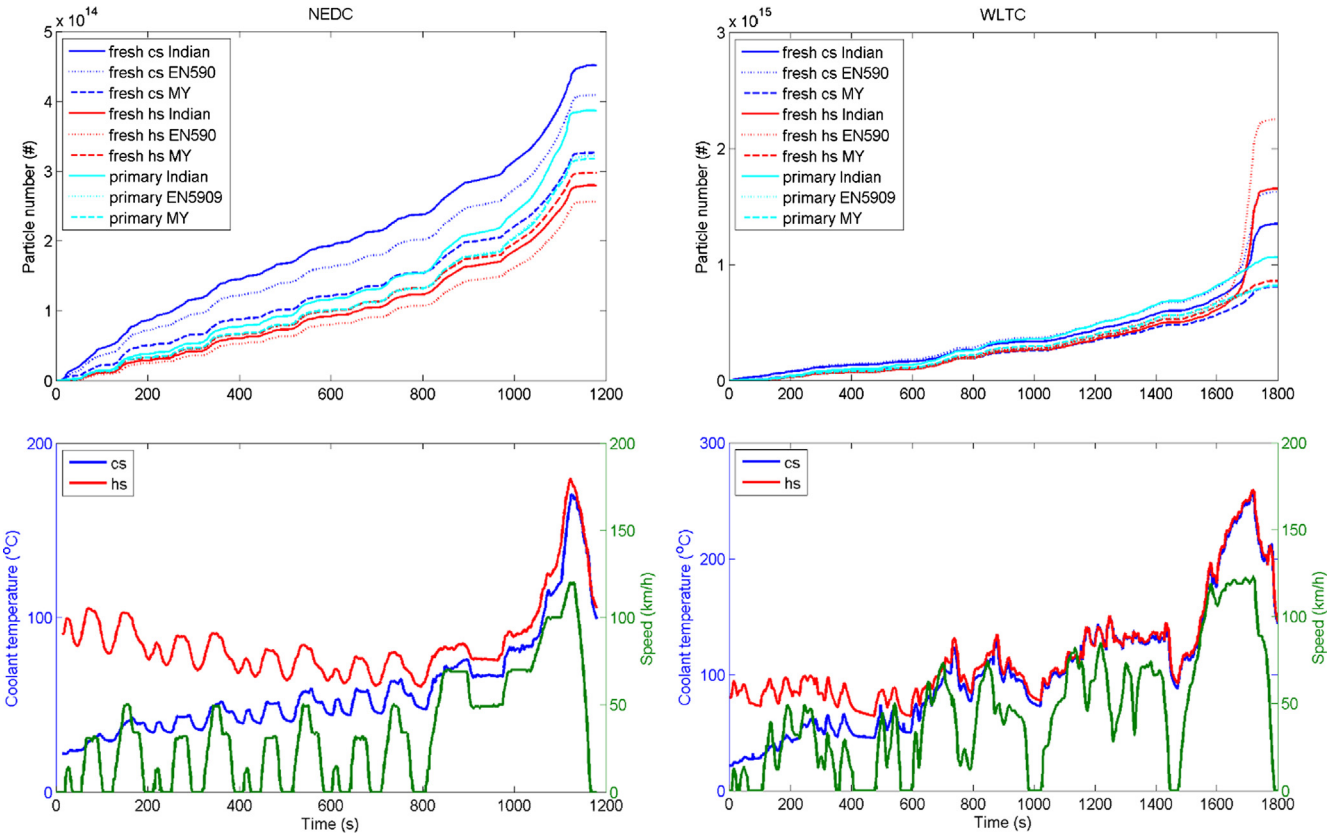

Fig. 3. Cumulative particle emissions (a)–(b) together with coolant temperatures (blue curve for cold start, red curve for hot start) and vehicle speed (green curve) (c)–(d) for three used diesel fuels. The left side presents the NEDC cycle and the right side represents the WLTC cycle. Note different scales of the vertical axes. Note that cs and hs refer to cold start and hot start cycles, respectively.

4. Results and discussion

4.1. Particle number emissions during the NEDC and WLTC cycles

Fig. 2 presents the time series of the vehicle speed and number of particles larger than 2.5 nm emitted over the NEDC and WLTC cycles for the diesel vehicle fuelled by Indian diesel BS IV (see Supporting Information Fig. S1 for the other fuels). The results are presented for the primary exhaust particles measured downstream of the double-ejector dilution system as well as for the fresh exhaust measured downstream from the porous tube dilution system for the fresh cs and fresh hs cycles.

For all fuels, driving conditions were observed to strongly affect exhaust emissions. Fig. 2 for the Indian diesel and Fig. S1 for the MY and EN590 diesels show that during the NEDC and WLTC cycles, the emissions had similar characteristics, but some notable deviations were also observed. The peak emissions occurred at accelerations and decelerations during engine braking. However, due to more aggressive acceleration, the peak emissions were higher during the WLTC. Consequently (and also due to the longer duration of the WLTC), the cumulative particle number emissions at the end of the cold and hot WLTC cycles were much higher than the ones measured in the NEDC; for example, two and five times higher for the Indian fuel (Fig. 3).

High exhaust particle emissions occurred during the last acceleration in the EUDC part of the NEDC and the extra-high speed phase of the WLTC (Figs. 2 and 3). In the EUDC, the primary and fresh emissions were rather similar, indicating that these particles were non-volatile and already existed in the tailpipe. On the contrary, the primary particle emissions were much lower than the fresh particle emissions (hs) during the extra-high speed phase, indicating that most of these particles were volatile and formed when the exhaust was cooled from the elevated tailpipe temperature (Fig. 3) to the room temperature. Note that the dilution air temperature of the PTD was approximately 30 °C in the measurements of fresh exhaust. Comparing the primary and fresh exhaust particle concentrations, about 67, 84 and 23% of the particles (> 2.5 nm) for the Indian diesel, EN590 and MY diesel, respectively, in the extra-high speed phase were volatile. It should be noted that the fresh emissions might be underestimated since losses onto the walls of the ageing chamber in the PTD cannot be taken exactly into account, due to the partly unknown dynamics of volatile nanoparticle formation.

The observed particle number emission factors EF_N (#/km) for all fuels were systematically larger over the WLTC than over the NEDC (Table 1). Considering the fresh exhaust emissions, the highest observed emission factor over the WLTC was 1.0×10^{14} #/km for the EN590 diesel, and over the NEDC it was 2.7×10^{13} #/km for the MY diesel. The greatest difference between the driving cycles was observed for the EN590 fuel for which the ratio of the emission factors (WLTC/NEDC) were 1.9 and 4.3 for the fresh exhaust cold start and hot start cycles, respectively, whereas they were 1.5 and 2.9 for the Indian diesel, and 1.2 and 1.4 for the MY diesel. The main reason for this behavior is the high EF_N for EN590 during the extra-high speed phase of the WLTC as given in Table 1 and Fig. S2(b).

Regarding the primary exhaust, the highest particle number emission factors were obtained for the Indian diesel over the NEDC (3.6×10^{13} #/km) and over the WLTC (4.8×10^{13} #/km) as well as also over all the phases of both cycles (Table 1 and Fig. S2c). The relatively high primary particle number emissions with the Indian diesel seems to be caused by the highest soot/BC emissions (see below), and the reason for those might be the highest aromatic hydrocarbon content of the Indian diesel (Table S2).

4.2. Particle size distributions during the NEDC and WLTC cycles

As an example, Fig. 4 depicts the time series of particle number size distributions (particles in the size range of 5.6–560 nm) for the fresh exhaust emissions (both cold and hot start cycles) and primary exhaust emissions with the EN590. The other cases are presented in Fig. S3.

During the first 200 s of the NEDC and WLTC cold start cycles (Fig. 4a and d) the fresh emissions of particles > 30 nm were clearly higher than during the hot start cycles (Fig. 4b and e). In both cycles the smaller particles (< 20 nm) were emitted during acceleration and deceleration, particularly during the extra-high phase of the WLTC. Since the majority of these smallest particles cannot be observed in the primary emissions during the extra-high phase (Fig. 4f), the particles have been formed in the sampling system used to study fresh exhaust emissions (i.e., during the rapid cooling and dilution of exhaust). This indicates that these smallest particles could be of sulfuric acid origin [34], thus they are likely also affected by the fuel sulfur content. However, although the FSC was higher in the Indian diesel than in the EN590, relatively similar emissions were observed when these fuels were used (Fig. S3). Instead, equally high nanoparticle emissions were not observed in the fresh exhaust when the vehicle was fuelled with the sulfur-free MY diesel.

During accelerations and high-speed driving, the primary particle size distributions were typically dominated by soot mode particles (i.e., particles in sizes larger than 10–20 nm). Instead, during deceleration conditions, the particle size distributions were shifted to smaller particle sizes, and the role of the sub-10 nm particles became much more significant (Fig. 4). Plausibly they were formed during engine braking, and their origin was from the lubricant oil [16,20]. It should be noted that with all fuels, the primary exhaust nanoparticles were also emitted during the extra-high speed phase of the WLTC, meaning that especially with the EN590 and Indian diesels, the resultant fresh exhaust was externally mixed with two types of nanosized particles. Furthermore, particle size distribution measurements showed that with the MY diesel (Fig. S3), the sizes of the soot particles emitted during acceleration conditions were smaller than with the other fuels.

The average fresh particle (hot start) size distributions for particle number (#/km) and volume (cm^3/km) emissions over the different phases of the NEDC and WLTC cycles are presented in Fig. S4 and the distributions over the whole cycles in Fig. 5. Since the EEPS data were not available for the Indian diesel during the NEDC cycle, the results concerning the NEDC particle number size distributions are presented based on the ELPI data. However, the results concerning the WLTC are shown based on the both ELPI and EEPS data since the EEPS has better size resolution in the smaller sizes. To enable comparisons of the particle volume emissions, all of them were calculated from the ELPI data. With the MY diesel during the UDC (Fig. S4) and over the whole NEDC (Fig. 5), the number emissions of 6–100 nm particles were larger than with EN590 and Indian diesels, but the observed particle sizes were smaller. With the MY diesel, the soot mode peaked at ~40 nm, whereas

Table 1
Primary and fresh exhaust number emission factors of particles larger than 2.5 nm (EF_N, #/km) for the MY diesel, the standard diesel EN590, and the Indian diesel BS IV over the NEDC and WLTC cycles and over the different phases (Section 3.2). Note that cs and hs refer to cold and hot start, respectively.

			NEDC		WLTC			
EF_N ($\times 10^{13}$ #/km)	NEDC	WLTC	UDC	EUDC	Low	Medium	High	Extra-high
MY diesel								
fresh cs	2.99	3.63	3.90	2.48	3.69	3.20	3.30	4.14
fresh hs	2.73	3.86	3.36	2.38	3.68	3.55	3.82	4.13
primary	2.92	3.67	3.34	2.67	3.72	4.00	3.99	3.18
EN590 diesel								
fresh cs	3.76	7.31	5.10	2.99	5.98	4.16	4.55	11.96
fresh hs	2.36	10.12	2.71	2.15	3.61	3.93	4.08	21.22
primary	2.96	3.65	3.31	2.75	3.45	3.66	3.98	3.45
BS IV diesel								
fresh cs	4.14	6.07	6.01	3.09	5.49	3.77	3.95	9.40
fresh hs	2.57	7.44	3.12	2.26	3.27	3.58	3.59	14.47
primary	3.55	4.77	3.89	3.36	4.50	4.85	4.89	4.73

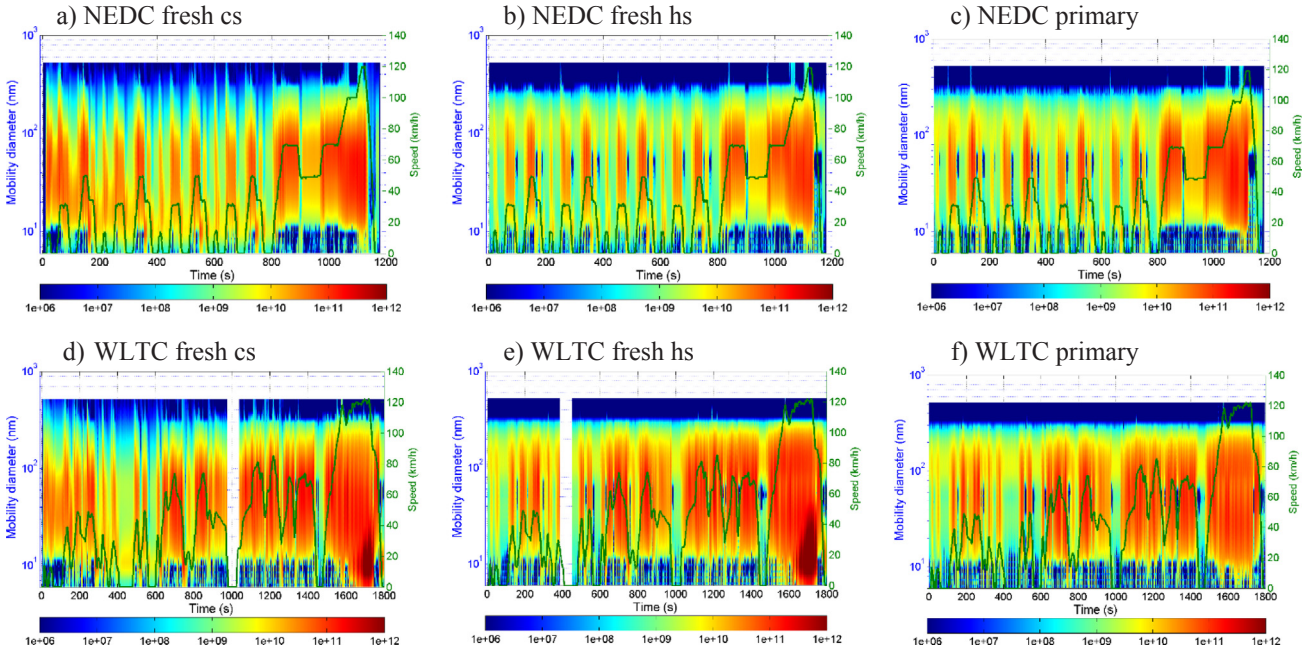

Fig. 4. Time series of the size distributions of the exhaust particle number emissions (#/s) along with the vehicle speed during the NEDC (a–c) and WLTC (d–f) cycles with the EN590 diesel. Particles in the size range of 5.6–560 nm were measured by the EEPS. Shown are the size distributions for the fresh emissions cold start cycles (a, d) and hot start cycles (b, e), as well as for the primary emissions (c, f). The particle emissions are indicated by the color scale and the vehicle speed by the green curve.

with the other fuels the soot modes peaked at ~70 nm. Additionally, the number emissions of > 100 nm particles with the MY diesel were less than for the EN590 and Indian fuels. Due to the smaller particle sizes it is not surprising that the particle volume emissions were lowest for the MY diesel and highest for the Indian diesel (Figs. 5 and S4).

Over the WLTC, more differences in the particle number size distributions can be observed between the fuels, and in general the emissions were clearly higher when compared to those over the NEDC. During the low-, medium- and high-speed phases (Fig. S4), the size of the soot mode from the MY diesel was smaller than from the other fuels; the mode peaked at ~55 nm (mobility diameter), whereas with the Indian diesel the soot mode peaked at ~60 nm, and with the EN590 diesel the mode peaked at 55 nm and 100 nm at the low phase and at ~60 nm for the medium and high phases. Additionally, in the particle number size distribution a nucleation mode peaking at ~11 nm is evident during the extra-high phase and during the whole WLTC with the EN590 and Indian fuels (Figs. 5 and S4).

As to the particle volume emissions, the emissions over the WLTC were almost two times the emissions over the NEDC. The highest emissions were measured for the EN590 fuel and lowest for the renewable MY diesel. As explained earlier, the larger soot mode and thus the larger particle volume emissions with the Indian diesel and EN590 can be explained by the higher aromatic hydrocarbon content of the fuels (Table S2).

4.3. NOx emissions

The NOx emissions from the studied vehicle behaved in a relatively similar way as the total particle emissions; at the beginning of the cycles, the cold start emissions were somewhat higher compared to the hot start cycles, and high peaks occurred during the last acceleration of the NEDC and during the extra-high speed phase of the WLTC (Fig. S5). The NOx emission factors for the NEDC were 138–205 mg/km (Table 2), and the highest emission factors were obtained with the EN590. However, with all fuels the factors were below the Euro 4 standard (250 mg/km), and for the MY diesel and Indian diesel the NOx emissions were even below the Euro 5 standard (180 mg/km), but still far from the Euro 6 standard of 80 mg/km. However, the NOx emission factors depended on the test cycle; under the WLTC they were considerably higher compared to the NEDC, being in the range of 264–360 mg/km in hot start cycles. Interestingly, for the Indian diesel the NOx emissions were higher in cold start cycles but for the MY diesel they were lower, possibly resulting from differences in fuel properties. Compared to this study, Marotta et al. [42] reported somewhat higher average NOx emissions of nine diesel passenger cars (Euro 4–6), 217 ± 21 mg/km and 391 ± 171 mg/km under the NEDC and WLTC, respectively, whereas Suarez-Bertoa et al. [68] reported the values of 184 mg/km and 458 mg/km for two studied diesel cars (Euro 5–6) over the WLTC. On the other hand, Ko et al. [46] reported that the NOx emissions from a Euro 6 compliant diesel passenger car equipped with a lean NOx trap exceeded the regulatory limit by approximately 17 mg/km in the WLTC at 23 °C but met the limit in the NEDC. It should be noted that in our study the cumulative emissions of NOx (Fig. S6) significantly increased during the extra-high phase of the WLTC, even to 2–3-fold when the vehicle speed increased from 80 km/h to 120 km/h. Typically, EF_{NO} was around 30–35% of EF_{NOx} in the WLTC and slightly higher, around 40%, in the NEDC. As shown in Table 2, the NOx emission factors were higher in the urban areas (UDC and low speed phase of the WLTC) where the average speed is 18–19 km/h due to stop and go driving (Table S3) compared to the EUDC and medium–high speed phases of the WLTC. However, the emission factors were much higher in the extra-high phase.

4.4. Chemical composition of primary and fresh particle emissions

4.4.1. Time series of BC, sulfate and organics

Fig. 6 shows the time series of the BC emissions in the NEDC (a) and in the WLTC (b) for the Indian diesel, based on the aethalometer data measured with the wavelength of 880 nm. This wavelength has been observed to be the most suitable wavelength to measure the light-absorbing soot originating from traffic [69,70]. BC emissions for other fuels can be seen in Fig. S7. In general, the BC emissions were associated with acceleration conditions, and regarding the steady driving situations of the NEDC, they increased when the vehicle speed

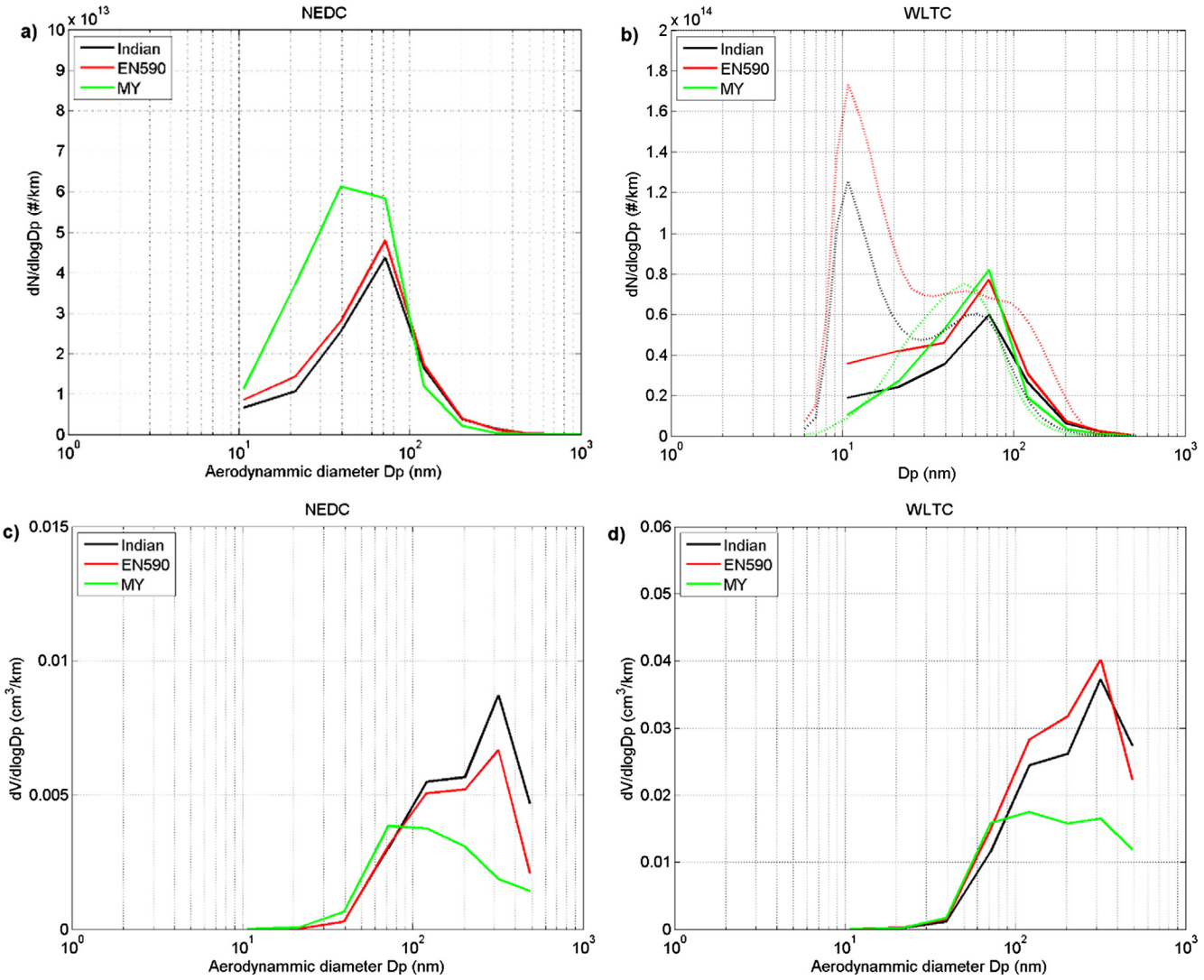

Fig. 5. Average size distributions of fresh (hot start) particle number (#/km) (a)–(b) and volume (cm^3/km) (c)–(d) of emissions for different fuels over the NEDC and WLTC cycles. The size distributions were measured with the ELPI (solid curves). Furthermore, the particle number size distributions were measured with the EEPS over the WLTC (dotted curves in b). Idle emissions are also included. The average speed over the NEDC was 33.4 km/h and over the WLTC it was 46.5 km/h. Note the different scales of the vertical axes.

increased. In the middle of the NEDC, minor BC emission peaks were also observed during deceleration conditions or short steady speed periods between them.

The WLTC is more aggressive than the NEDC (i.e., it contains more speed changes). This results in higher BC emissions, especially at the end of the cycle. In general, the temporal behavior of the BC emissions was very similar with the soot mode particle emissions seen in Fig. 4.

Fig. 7 presents the temporal behavior of sulfate and organic compounds in the particulate matter of the fresh exhaust. The results are shown for the Indian diesel and MY diesel. In regard to sulfate, for both

Table 2
Emission factors (mg/km) of NO and NOx during the NEDC and WLTC for different fuels. Note that the emission factors of NOx during the different segments of the NEDC and WLTC are also shown; cs and hs refer to cold and hot start cycles, respectively.

	NO		NOx		NEDC		WLTC			
EF (mg/km)	NEDC	WLTC	NEDC	WLTC	UDC	EUDC	low	medium	high	extra-high
MY diesel										
fresh cs	58	122	141	282	167	127	229	146	132	506
fresh hs	53	135	172	360	193	161	262	193	173	652
EN590										
fresh cs	80	127	205	336	247	182	256	174	169	599
fresh hs	54	120	182	343	205	170	260	180	164	619
BS IV diesel										
fresh cs	59	138	143	338	154	137	389	157	150	581
fresh hs	41	94	138	264	147	134	184	139	122	487

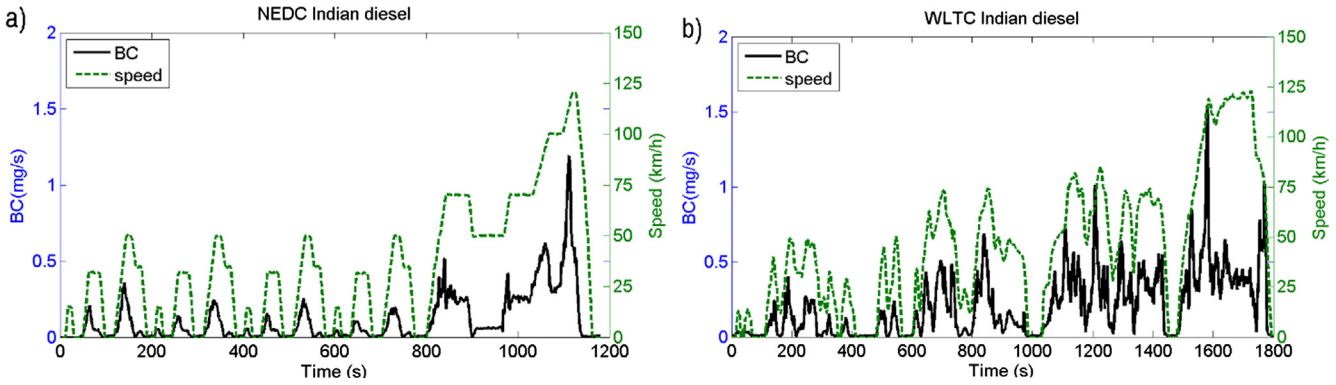

Fig. 6. Primary BC emissions during the NEDC (a) and WLTC (b) for the Indian fuel.

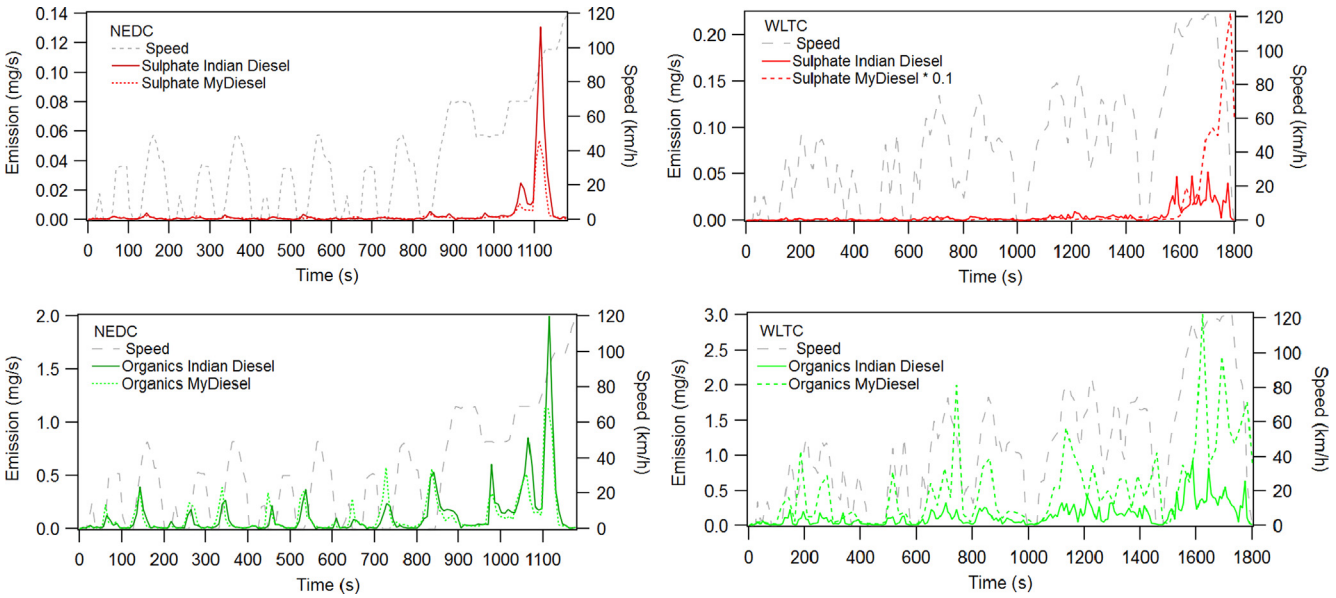

Fig. 7. Time series of hot start emission of fresh exhaust particulate sulfate and organics over the NEDC (left panels) and over the WLTC (right panels) for the Indian diesel and MY diesel. The vehicle speed is also shown. Note that sulfate emissions for MY diesel over the WLTC were multiplied by 0.1.

cycles and fuels the emissions were mostly observed during the high-speed conditions (when the vehicle speed was > 80 km/h). Due to the low FSC of MY diesel (< 1 ppm) it is assumed that these sulfate emissions are more related to lubricant oil than fuel. This lubricant oil hypothesis is supported by the results of Timonen et al. [71] who also observed sulfate emissions for alcohol fuels. This result is also in line with the results of Carbone et al. [72] who showed that large fraction of a diesel engine emissions originated from the lubricant oil. Additionally in this study, we observed that the emissions of particulate zinc relatively closely followed the sulfate emissions (Fig. S8). Pirjola et al. [35], for instance, found a positive correlation of the Zn concentration in the lubricant oil with non-volatile particle number emission factors during the NEDC, and on the other hand, the non-volatile particles correlated positively with the lubricant oil sulfur. However, we note that sulfur compounds may also experience partial storage in the DOC of the studied vehicle at low exhaust temperatures and then eventually be released at higher temperatures. Consequently, the driving history and the consequent storage–release effect cannot be totally ruled out. Organic matter concentrations seem to be mostly correlated with accelerations for both cycles. The highest organic particulate matter

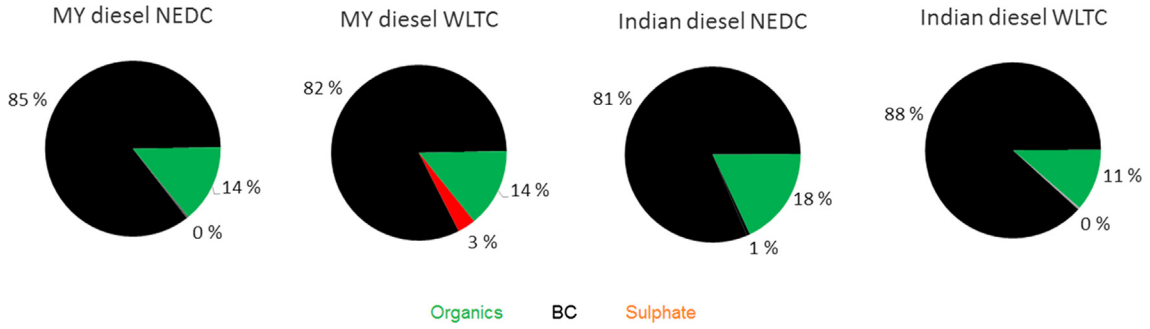

Fig. 8. Chemical compositions of the fresh exhaust emissions over the NEDC and WLTC hot start cycles for the MY diesel and Indian diesel.

emissions, measured from the fresh exhaust, were observed at the highest speeds at the end of the cycle for both NEDC and WLTC.

4.4.2. Emission factors for BC

Fig. S9 presents average emission factors for primary and fresh BC and BrC (brown carbon), calculated from the aethalometer data (880 nm and 370 nm). Due to technical issues, the data for the MY diesel are missing during the cold start of the WLTC. For BC and BrC, the emission factors were lowest for the MY diesel (7.8–15 mg/km) and slightly higher for EN590 (7.6–17.7 mg/km), and the highest EFs (7.6–21.6 mg/km) were observed for the Indian diesel. In fact, the EF_{BC} was ~20% lower for MY compared to EN590, and ~29–40% lower compared to the Indian diesel. For all fuels the EF_{BcC} were on average 20% higher than the EF_{BC}. Typically the cold start EFs for BC and BrC were higher than the hot start EFs. With an exception of the NEDC for the MY diesel, the EFs for the primary emissions were higher than for fresh hs emissions (Fig. S9).

Fig. 8 represents the relative contribution of different main chemical compounds (BC, organics and sulfate) over the NEDC and WLTC cycles for the MY diesel and Indian diesel. The composition is clearly dominated by the BC (81–88%) with some contribution from organics (11–18%) and sulfate (0–3%). Similarly, Maricq [73] measured PM from diesel and gasoline vehicles of model years 2012–2013 and observed these vehicles exhibiting a high (> 80%) BC fraction. In general, the particulate exhaust emissions of a diesel vehicle without a DPF mainly consist of BC and some minor fraction of organic compounds and sulfates [28,32]. With the DPF, most of the BC emissions are removed and contribution of organics and sulfate to total PM increases, but the amount of particulate emissions significantly decreases. However, regardless of a DPF, elevated BC emissions have been observed in certain conditions including e.g. cold start [37] and DPF regeneration [33].

5. Conclusions

In this study the emissions of NOx and particles for a Euro 4 diesel vehicle, representative of a diesel passenger car in India, were determined. Regarding the particle emissions, we studied the size distributions, chemical composition, and mass and number concentrations of exhaust particles. The measurements were made using three fuels with significantly different characteristics: (i) Indian diesel fuel (BS IV) with relatively high fuel sulfur and aromatic content, (ii) European low sulfur diesel fuel (EN590) with relatively high aromatic content, and (iii) sulfur and aromatic free renewable diesel (MY diesel). The emissions were characterized over the standardized test cycles NEDC and WLTC whose driving patterns significantly differ from each other. The emission factors for NOx and particles were also calculated.

The major conclusions drawn from our present investigations are as follows.

- The lowest primary particle BC emissions were measured when MY diesel was used, for which the BC emissions were 17% and 29% lower compared to the use of EN590 and Indian diesel, respectively. This result, based on the aethalometer data, was in line with particle volume size distributions that indicated the lowest volume concentration in particle sizes larger than 100 nm for the renewable fuel for both test cycles and in all segments of those cycles. Lower BC emissions for the renewable fuel may likely be caused by its low aromatic content, but other fuel or combustion parameters may also have effects on BC emission formation.
- For all the fuels, exhaust particle composition measurements revealed that most of the fresh exhaust particulate mass emissions consisted of BC (81–88%), and clearly a minor fraction was organic compounds (11–18%) and sulfate (0–3%). This was also indicated by the number size distributions, dominated by the non-volatile particles in the typical soot particle size range.
- The instantaneous particle emissions depended strongly on the driving situation. In general, the highest BC emissions were observed during accelerations, mostly originated from soot formation in the fuel combustion process.
- Instantaneous peaks of high particle emissions were observed also during decelerations, especially in UDC parts of the NEDC cycle. These were associated with the emissions of sub-10 nm particles, seen also in the primary particles, which indicates different origins of the particles. These nanoparticles were observed to contain non-volatile compounds and were most likely formed from lubricant-oil-originated compounds. During motoring, no fuel injection or combustion process exists in cylinders.
- Furthermore, high concentrations of nanoparticles in high-speed conditions were clearly observed with Indian diesel and EN590 diesel but not with the sulfur- and aromatic-free renewable MY diesel. These nanoparticles were observed to consist of volatile material. We interpret the result as being linked to fuel sulfur content and to sulfur-driven nucleation of new particles in cooling dilution of exhaust.
- The particle emissions were significantly higher during the WLTC; the difference was seen in all the emission factors reported above (i.e., in the particle number emissions, BC emissions, and in total particulate mass emissions). For example, the fresh exhaust number emission factor for particles larger than 2.5 nm varied in the range of 2.4×10^{13}–2.7×10^{13} #/km over the NEDC, whereas during the WLTC, they were in the range of 3.9×10^{13}–1.0×10^{14} #/km, the lowest value was obtained with the MY diesel. In the regulatory emission testing of passenger cars, the WLTC is replacing the NEDC. Compared to the NEDC, the WLTC is more aggressive in respect to accelerations and decelerations, and it has been designed to correspond better to the real driving conditions of vehicles. It is important to note that the observed difference may indicate that real particle emissions of diesel passenger cars, especially regarding the technology level currently used in India, are higher than indicated before.

Although the use of DPFs is the most effective technology to control particle emissions, and already is quite commonly used in Europe and North America in new vehicles, the countries with less restrictive emission legislation, e.g. in Asia and southern America, still have a large number of diesel vehicles without DPF. As the renewal of vehicle fleet is slow (more than a decade), one reasonable alternative to mitigate the GHG and soot emissions could be the replacement of fossil fuels to the renewable biofuel in the transport sector. The results of this study regarding the effects of fuels and driving conditions on vehicular exhaust can be used in more efficient and modernized traffic regulations in developing countries to tackle their urban air quality problems. The renewable MY diesel is a commercial product that is suitable for all diesel engines. It satisfies the greenhouse gas and sustainability requirements. Moreover, to develop new low emissions and environment friendly fuels for traffic is a part of the development of the global sustainable energy system.

Acknowledgements

This work was a part of the Traffic and Air Quality in India: Technologies and Attitudes (TAQIITA) project and was funded by Business Finland; Department of Biotechnology, India; Dekati Oy; Pegasor Oy; Neste; and Helsinki Region Environmental Services Authority (HSY). The authors are very grateful to Aleksi Malinen and Sami Kulovuori from the Metropolia University of Applied Sciences for technical expertise and operation of the dynamometer, as well as to Niina Kuittinen and Matti Lassila from Tampere University for assisting in the measurements.

Appendix A. Supplementary material

Supplementary data to this article can be found online at https://doi.org/10.1016/j.apenergy.2019.113636.

References

[1] IPCC report 2018. https://www.ipcc.ch/sr15/ [assessed 27 May 2019].
[2] Bond TC, Doherty SJ, Fahey DW, Forster PM, Berntsen T, DeAngelo BJ, et al. Bounding the role of black carbon in the climate system: a scientific assessment. J Geophys Res [Atmos] 2013;118:5380–552.
[3] Behrentz E, Ling R, Rieger P, Winer AM. Measurements of nitrous oxide emissions from light-duty motor vehicles: a pilot study. Atmos Environ 2014;38:4291–303.
[4] International Energy Agency, 2019. https://www.iea.org/statistics/co2emissions/ [assessed 27 May 2019].
[5] Pope III CA, Dockery DW. Health effects of fine particulate air pollution: lines that connect. J Air Waste Manag Assoc 2006;56:707–42.
[6] Sioutas C, Delfino RJ, Singh M. Exposure assessment for atmospheric ultrafine particles (UFPs) and implications in epidemiologic research. Environ Health Perspect 2005;113:947–55.
[7] Kettunen J, Lanki T, Tiittanen P, Aalto PP, Koskentalo T, Kulmala M, et al. Associations of fine and ultrafine particulate air pollution with stroke mortality in an area of low air pollution levels. Stroke 2007;38:918–22.
[8] Su DS, Serafino A, Müller JO, Jentoft RE, Schlögl R, Fiorito S. Cytotoxicity and inflammatory potential of soot particles of low-emission diesel engines. Environ Sci Technol 2008;42:1761–5.
[9] Jacobs L, Nawrot TS, de Geus B, Meeusen R, Degraeuwe B, Bernard A, et al. Subclinical responses in healthy cyclists briefly exposed to traffic-related air pollution: an intervention study. Environ Health 2010;9:64.
[10] Agarwal AK, Singh AP, Gupta T, Agarwal RA, Sharma N, Rajput P, et al. Mutagenicity and cytotoxicity of particulate matter emitted from biodiesel-fueled engines. Environ Sci Technol 2018;52:14496–507.
[11] Cheung KL, Ntziachristos L, Tzamkiozis T, Schauer JJ, Samaras Z, Moore KF, et al. Emissions of particulate trace elements, metals and organic species from gasoline, diesel, and biodiesel passenger vehicles and their relation to oxidative potential. Aerosol Sci Technol 2010;44:500–13.
[12] Kittelson DB. Engines and nanoparticles: a review. J Aerosol Sci 1998;29:575–88.
[13] Tobias H, Beving D, Ziemann P, Sakurai H, Zuk M, McMurry P, et al. Chemical analysis of diesel engine nanoparticles using a nano-DMA/thermal desorption particle beam mass spectrometer. Environ Sci Technol 2001;35:2233–43.
[14] Sakurai H, Tobias H, Park K, Zarling D, Docherty K, Kittelson D, et al. On-line measurements of diesel nanoparticle composition and volatility. Atmos Environ 2003;37:1199–210.
[15] Rönkkö T, Virtanen A, Kannosto J, Keskinen J, Lappi M, Pirjola L. Nucleation mode particles with a non-volatile core in the exhaust of a heavy duty diesel vehicle. Environ Sci Technol 2007;41:6384–9https://pubs.acs.org/doi/abs/10.1021/es0705339.
[16] Rönkkö T, Pirjola L, Ntziachristos L, Heikkilä J, Karjalainen P, Hillamo R, et al. Vehicle engines produce nanoparticles even when not fuelled. Environ Sci Technol 2014;48:2043–50.
[17] Filippo A, Maricq M. Diesel nucleation mode particles: semivolatile or solid? Environ Sci Technol 2008;42:7957–62.
[18] Rönkkö T, Lähde T, Heikkilä J, Pirjola L, Bauschke U, Arnold F, et al. Effect of gaseous sulfuric acid on diesel exhaust nanoparticle formation and characteristics. Environ Sci Technol 2013;47:11882–9. https://doi.org/10.1021/es402354y.
[19] Kittelson DB, Watts WF, Johnson JP, Thorne C, Higham C, Payne JR, et al. Effect of fuel and lube oil sulfur on the performance of a diesel exhaust gas continuously regenerating trap. Environ Sci Technol 2008;42:9276–82.
[20] Karjalainen P, Pirjola L, Heikkilä J, Lähde T, Tzamkiozis T, Ntziachristos L, et al. Exhaust particles of modern gasoline vehicles: a laboratory and an on-road study. Atmos Environ 2014;97:262–70.
[21] Arnold F, Pirjola L, Aufmhoff H, Schuck T, Lähde T, Hämeri K. First gaseous sulfuric acid measurements in automobile exhaust: Implications for volatile nanoparticle formation. Atmos Environ 2006;40:7097–105.
[22] Arnold F, Pirjola L, Rönkkö T, Reichl U, Schlager H, Lähde T, et al. First on-line measurements of sulfuric acid gas in modern heavy duty diesel engine exhaust: Implications for nanoparticle formation. Environ Sci Technol 2012;46:11227–34.
[23] Kumar P, Ketzel M, Vardoulakis S, Pirjola L, Britter R. Dynamics and dispersion modelling of nanoparticles from road traffic in the urban atmospheric environment – a review. J Aerosol Sci 2011;42:580–603.
[24] Shi J, Harrison R. Investigation of ultrafine particle formation during diesel exhaust dilution. Environ Sci Technol 1999;33:3730–6.
[25] Schneider J, Hock N, Weimer S, Borrmann S, Kirchner U, Vogt R, et al. Nucleation particles in diesel exhaust: composition inferred from in situ mass spectrometer analysis. Environ Sci Technol 2005;39:6153–61.
[26] Khalek IA, Spears M, Charmley W. Particle size distribution from heady-duty diesel engine: Steady-state and transient emission measurement using two dilution systems and two fuels. SAE technical paper series 2003; 2003-01-0285.
[27] Kroll JH, Smith JD, Worsnop DR, Wilson KR. Characterisation of lightly oxidised organic aerosol formed from the photochemical aging of diesel exhaust particles. Environ Chem 2012;9:211–20.
[28] Chirico R, DeCarlo PF, Heringa MF, Tritscher T, Richter R, Prévôt ASH, et al. Impact of aftertreatment devices on primary emissions and secondary organic aerosol formation potential from in-use diesel vehicles: results from smog chamber experiments. Atmos Chem Phys 2010;10:11545–63. https://doi.org/10.5194/acp-10-11545-2010.
[29] DieselNet; 2019. https://www.dieselnet.com/standards/eu/ld.php [assessed 27 May 2019].
[30] Maricq M, Chase R, Xu N, Laing P. The effects of the catalytic converter and fuel sulfur level on motor vehicle particulate matter emissions: light duty diesel vehicles. Environ Sci Technol 2002;36:283–9.
[31] Holmén B, Ayala A. Ultrafine PM emissions from natural gas, oxidation-catalyst diesel, and particle-trap diesel heavy-duty transit buses. Environ Sci Technol 2002;36:5041–50.
[32] Maricq MM. Chemical characterization of particulate emissions from diesel engines: a review. J Aerosol Sci 2007;38. 1079–1118.ordon.
[33] Gordon TD, Pesto AA, Nguyen NT, Robertson WH, Na K, Sahay KN, et al. Secondary organic aerosol production from diesel vehicle exhaust: impact of aftertreatment, fuel chemistry and driving cycle. Atmos Chem Phys 2014;14:4643–59. https://doi.org/10.5194/acp-14-4643-2014.
[34] Vaaraslahti K, Keskinen J, Giechaskiel B, Solla A, Murtonen T, Vesala H. Effect of lubricant on the formation of heavy-duty diesel exhaust nanoparticles. Environ Sci Technol 2005;39:8497–504.
[35] Pirjola L, Karjalainen P, Heikkilä J, Saari S, Tzamkiozis T, Ntziachristos L, et al. Effects of fresh lubricant oil on particle emissions emitted by a modern GDI passenger car. Environ Sci Technol 2015;49:3644–52.
[36] Rönkkö T, Virtanen A, Vaaraslahti K, Keskinen J, Pirjola L, Lappi M. Effect of dilution conditions and driving parameters on nucleation mode particles in diesel exhaust: laboratory and on-road study. Atmos Environ 2006;40:2893–901.
[37] Suarez-Bertoa R, Astorga C. Impact of cold temperature on Euro 6 passenger car emissions. Environ Pollut 2018;234:318–29. https://doi.org/10.1016/j.envpol.2017.10.096.
[38] Burtscher H. Physical characterization of particulate emissions from diesel engines: a review. J Aerosol Sci 2005;36:896–932.
[39] Myung CL, Ko A, Park S. Review on characterization of nano-particle emissions and PM morphology from internal combustion engines: Part 1. Int J Automot Technol 2014;15:203–18.
[40] Choi S, Myung CL, Park S. Review on characterization of nano-particle emissions and PM morphology from internal combustion engines: Part 1. Int J Automot Technol 2014;15:219–27.
[41] Bielaczyk P, Woodburn J, Szczotka A. A comparison of carbon dioxide exhaust emissions and fuel consumption for vehicles tested over the NEDC, FTP-75 and WLTC chassis dynamometer test cycles. SAE technical paper 2015; 2015-01-1065. http://doi.org/10.4271/2015-01-1065.
[42] Marotta A, Pavlovic J, Ciuffo B, Serra S, Fontaras G. Gaseous emissions from light-duty vehicles: moving from NEDC to the new WLTP test procedure. Environ Sci Technol 2015;49:6315–22.
[43] Pavlovic J, Marotta A. Ciuffo B CO_2 emissions and energy demands of vehicles tested under the NEDC and the new WLTP type approval test procedures. Appl Energy 2016;177:661–70.
[44] Tsokolis D, Tsiakmakis S, Dimaratos A, Fontaras G, Pistikopoulos P, Ciuffo B, et al. Fuel consumption and CO_2 emissions of passenger cars over the New Worldwide Harmonized Test Protocol. Appl Energy 2016;179:1152–62.
[45] Giakoumis EG, Zachiotis AT. Investigation of a diesel-engined vehicle's performance and emissions during the WLTC driving cycle – comparison with the NEDC. Energies 2017;10:240–59. https://doi.org/10.3390/en10020240.
[46] Ko J, Jin D, Jang W, Myung CL, Kwon S, Park S. Comparative investigation of NOx emissions characteristics from a Euro 6-compliant diesel passenger car over the NEDC and WLTC at various ambient temperatures. Appl Energy 2017;187:652–62.
[47] Arvidsson R, Persson S, Fröling M, Svanström M. Life cycle assessment of hydrotreated vegetable oil from rape, oil palm and Jatropha. J Cleaner Prod 2011;19:129–37.
[48] Rose L, Hussain M, Ahmed S, Malek K, Costanzo R, Kjeang E. A comparative life cycle assessment of diesel and compressed natural gas powered refuse collection vehicles in a Canadian city. Energy Policy 2013;52:453–61.
[49] Edwards R, Larivé JF, Beziat JC. Well-to-wheels analysis of future automotive fuels and powertrains in the European context. JRC scientific and technical reports, well-to-wheels report, version 3c; July 2011.
[50] Rathore D, Nizami AS, Singh A, Pant D. Key issues in estimating energy and greenhouse gas savings of biofuels: challenges and perspectives. Biofuel Res J 2016;10:380–93. https://doi.org/10.18331/BRJ2016.3.2.3.
[51] Nylund N-O, Erkkilä K., Ahtiainen M, Murtonen T, Saikkonen P, Amberla A, et al. Optimized usage of NExBTL renewable diesel fuel. VTT research notes; 2011. 2604. https://www.vtt.fi/inf/pdf/tiedotteet/2011/T2604.pdf.
[52] Kopperaoinen A, Kytö M, Mikkonen S. Effect of hydrotreated vegetable oil (HVO) on particulate filters of diesel cars. SAE technical paper 2011. 2011.01.2096.
[53] Bartolomev CH. Mechanisms of catalyst deactivation. Appl Catal A: Gen 2001;212:17–60.
[54] Hartikka T, Kuronen M, Kiiski U. Technical performance of HVO (Hydrotreated Vegetable Oil) in diesel engines. SAE technical paper 2012. https://doi.org/10.4271/2012-01-1585. 2012-01-1585.
[55] Aatola H, Larmi M, Sarjovaara T, Mikkonen S. Hydrotreated vegetable oil (HVO) as a renewable diesel fuel: Trade-off between NOx, particulate emission, and fuel consumption of a heavy duty engine. SAE Int J Engines 2009;1:1251–62. https://doi.org/10.4271/2008-01-2500.
[56] Happonen M, Heikkilä J, Murtonen T, Lehto K, Sarjovaara T, Larmi M, et al. Reductions in particulate and NOx emissions by diesel engine parameter adjustments with HVO fuel. Environ Sci Technol 2012;46:6198–204. https://doi.org/10.1021/es300447t.
[57] Cordiner S, Mulone V, Novile M, Rocco V. Impact of biodiesel fuel on engine

emissions and aftertreatment system operation. Appl Energy 2016;164:972–83.
[58] Ntziachristos L, Giechaskiel B, Pistikopoulos P, Samaras Z, Mathis U, Mohr M, et al. Performance evaluation of a novel sampling and measurement system for exhaust particle characterization. SAE tech pap ser 2004; 2004-01-1439.
[59] Du H, Yu F. Nanoparticle formation in the exhaust of vehicles running on ultra-low sulfur fuel. Atmos Chem Phys 2008;8:4729–39. https://doi.org/10.5194/acp-8-4729-2008.
[60] Keskinen J, Rönkkö T. Can real-world diesel exhaust particle size distribution be reproduced in the laboratory? A critical review. J Air Waste Manage Assoc 2010;60:1245–55.
[61] Johnson T, Caldow R, Pöcher A, Mirme A, Kittelson D. A new electrical mobility particle sizer spectrometer for engine exhaust particle measurements. SAE technical papers 2004. https://doi.org/10.4271/2004-01-1341. 2004-01-1341.
[62] Keskinen J, Pietarinen K, Lehtimäki M. Electrical low pressure impactor. J Aerosol Sci 1992;23:353–60.
[63] Marjamäki M, Ntziachristos L, Virtanen A, Ristimäki Keskinen J, Moisio M, et al. Electrical filter stage for the ELPI. SAE tech pap 2002; 2002-01-0055.
[64] Yli-Ojanperä J, Kannosto J, Marjamäki M, Keskinen J. Improving the nanoparticle resolution of the ELPI. Aerosol Air Qual Res 2010;10:360–6.
[65] Onasch TB, Trimborn A, Fortner EC, Jayne JT, Kok GL, Williams LR, Davidovits P, Worsnop DR. Soot particle aerosol mass spectrometer: development, validation, and initial application. Aerosol Sci Technol 2012;46(7):804–17. https://doi.org/10.1080/02786826.2012.663948.
[66] DeCarlo PF, Kimmel JR, Trimborn A, Northway MJ, Jayne JT, Aiken AC, Gonin M, Fuhrer K, Horvath T, Docherty KS, Worsnop DR, Jimenez JL. Field-deployable, high-resolution, time-of-flight aerosol mass spectrometer. Anal Chem 2006;78(24):8281–9. https://doi.org/10.1021/ac061249n.
[67] Canagaratna MR, Jayne JT, Jimenez JL, Allan JD, Alfarra MR, Zhang Q, et al. Chemical and microphysical characterization of ambient aerosols with the aerodyne aerosol mass spectrometer. Mass Spectrom Rev 2007;26:185–222. https://doi.org/10.1002/mas.20115.
[68] Suarez-Bertoa R, Zardini AA, Lilova V, Meyer D, Nakatuni S, Hibel F, et al. Intercomparison of real-time tailpipe ammonia measurements from vehicles tested over the new world-harmonized light-duty vehicle test cycle (WLTC). Environ Sci Pollut Res 2015;22:7450–560.
[69] Helin A, Niemi J, Virkkula A, Pirjola L, Teinilä K, Backman J, et al. Characteristics and source apportionment of black carbon in the Helsinki metropolitan area. Finland. Atmos Environ 2018;190:87–98.
[70] Helin A, Virkkula A, Backman J, Pirjola L, Sippola O, Aakko-Saksa P, et al. Variation of absorption Ångström exponent in aerosols from different emission sources. Submitted to. J Geophys Res 2019.
[71] Timonen H, Karjalainen P, Saukko E, Saarikoski S, Aakko-Saksa P, Simonen O, et al. Influence of fuel ethanol content on primary emissions and secondary aerosol formation potential for a modern flex-fuel gasoline vehicle. Atmos Chem Phys 2017;17:5311–29.
[72] Carbone S, Timonen HJ, Rostedt A, Happonen M, Rönkkö T, Keskinen J, et al. Distinguishing fuel and lubricating oil combustion products in diesel engine exhaust particles. Aerosol Sci Technol 2019;53:594–607. https://doi.org/10.1080/02786826.2019.1584389.
[73] Maricq MM. Examining the relationship between black carbon and soot in flames and engine exhaust. Aerosol Sci Technol 2014;48:620–9. https://doi.org/10.1080/02786826.2014.904961.